Paper No. 380. (quote when citing this article)
Eleventh World Conference on Earthquake Engineering
ISBN: 0 08 042822 3

INTERACTION OF BOND DETERIORATION ALONG BEAM BARS THROUGH R/C INTERIOR JOINTS AND BEAMS

KITAYAMA Kazuhiro and JIANG Zhu

Department of Architecture, Faculty of Engineering, Tokyo Metropolitan University, Minami-Osawa 1-1, Hachioji-city, Tokyo, 192-03, Japan.

KOHYAMA Kouki

Kajima Corporation, Akasaka 6-5-30, Minato-ku, Tokyo, 107, Japan.

FURUTA Tomoki

Yahagi Construction, Aoi 3-19-7, Higashi-ku, Nagoya-city, Aichi, 461, Japan.

ABSTRACT

Reinforced concrete plane beam-column subassemblages consisted of a full-span beam, two half-span beams and two columns, a cruciform beam-column joint and an isolated beam were tested to study on the bond deterioration along beam longitudinal bars passing through an interior beam-column joint and a beam. The bond deterioration along beam bars within an interior beam-column joint and a beam influenced each other. The larger the slip of beam longitudinal bars within a joint was, the smaller that within a beam was. The beam bars through a frame could be developed at the compression side of a beam hinge region regardless of bond deterioration within both an interior beam-column joint and a center of a beam. The bond strength at the center of a beam was almost equal whether the beam bar ends were anchored or not.

KEYWORDS

Reinforced concrete; bond deterioration; beam bar; beam-column joint; slip.

INTRODUCTION

It is desirable to form the beam collapse mechanism in reinforced concrete (R/C) frames during earthquakes because plastic hinges developed at many beam ends can absorb well the energy induced by earthquake excitations without jeopardizing human life. Bond deterioration causing poor energy dissipation between concrete and longitudinal beam reinforcement passing through the interior beam-column joints and beam members should be avoided in such R/C frames. The relative slip of beam reinforcement to surrounding concrete occurs generally under cyclic reversed loading caused by earthquakes. Usual cruciform beam-column joints and isolated beam members have been tested solely for the research of beam bar bond characteristics. However beam longitudinal bars are arranged customarily through several spans of R/C frames. Such a specimen cannot reflect the interaction of bond deterioration along beam bars within an interior beam-column joint and a beam which may occur in actual R/C frames.

In order to study the interaction of bond deterioration along beam bars, three half-scale R/C subassemblages with beams framing into two columns, removed from a plane frame, were tested under horizontal load reversals. There are few studies using beam-column subassemblage specimens such as those used in this paper. Beam specimen with R/C stubs at beam ends, where beam longitudinal bars were anchored using 90-degree hooks, and an interior beam-column joint specimen were tested for comparison.

TEST PROGRAM

Three plane beam-column subassemblages consisted of a full-span beam, two half-span beams and two columns were tested; two subassemblages (Specimens M1 and M2) with the shear span of beams of 725 mm and one (Specimen L1) with that of 1225 mm. Beam longitudinal bars passing through subassemblage

specimens can move within beams and beam-column joints. Two other specimens were loaded for comparison. The cruciform beam-column joint (Specimen J1) was removed from Specimen M1 at the center of a full-span beam. Beam reinforcement in Specimen J1 was welded to the plates at the end of half-span beams. The beam of Specimen B was the same as the full-span beam of Specimen M2. Beam reinforcing bars in Specimen B, however, were anchored using 90-degree hooks in stubs at beam ends. The member sections and configurations of specimens are shown in Figs. 1 and 2. The properties of specimens are listed in Table 1. The dimensions of members were common in all specimens. Beam sections were 250x350 mm and column sections were 350x350 mm. The distance from bottom support of a column to the top horizontal loading point was 1720 mm. Specimens were designed to develop beam yielding and prevent joint shear failure by limiting joint input shear stress to 0.2 times the concrete compressive strength. Properties of steel and concrete are listed in Table 2. Concrete was cast in upright position so as to be done in actual frames.

The loading apparatuses are shown in Fig. 3. The beam ends of subassemblage specimens in Fig. 3(a) were supported by a horizontal roller, while the bottoms of the columns were supported by mechanical hinges. The horizontal reversed load was applied from the top of the column. Axial load on column was not applied for simplicity. The horizontal load applied by the jack and support reactions of half-span beams were measured by load-cells. The horizontal displacement at the top loading point of the column relative to the bottom hinge (called the story drift), beam and column deflections, joint shear distortion, beam end rotation and beam bar slip relative to the surrounding concrete were measured by strain-gauge type displacement transducers. Anti-symmetric bending at beam ends in Specimen B was applied by keeping two stubs parallel as shown in Fig. 3(b).

Specimens were subjected to nine and half loading cycles controlled using the story drift angle defined below; i.e., one cycle at the story drift angle of 1/400 rad, two cycles each at the story drift angle of 1/200, 1/100, 1/50 and 1/25 rad, and then to the story drift angle of 1/15 rad. Loading history of Specimen M2 in positive direction was changed to apply small displacement after an accident. The amplitude of beam deflection in each loading cycles for Specimen B was determined to be equal to that of Specimen M2 tested previously.

Table 1. Properties of specimens

Specimens	L1,M1,J1	M2	B
(a) Beam			
Longitudinal bars	5-D16	3-D22	
$a_t(mm^2)$	995	1,161	
$p_t(\%)$	1.24	1.52	
Stirrups	3-D10	2-D10	
@(mm)	120	120	
$p_w(\%)$	0.71	0.48	
(b) Column			
Total bars	12-D22		
$a_g(mm^2)$	4,644		
$p_g(\%)$	3.79		
Hoops	4-D10		
@(mm)	100		
$p_w(\%)$	0.81		
(c) Joint			
Hoops	4-D10		
Sets	3		
$a_w(mm^2)$	856		
P_{wj} (%)	0.84		

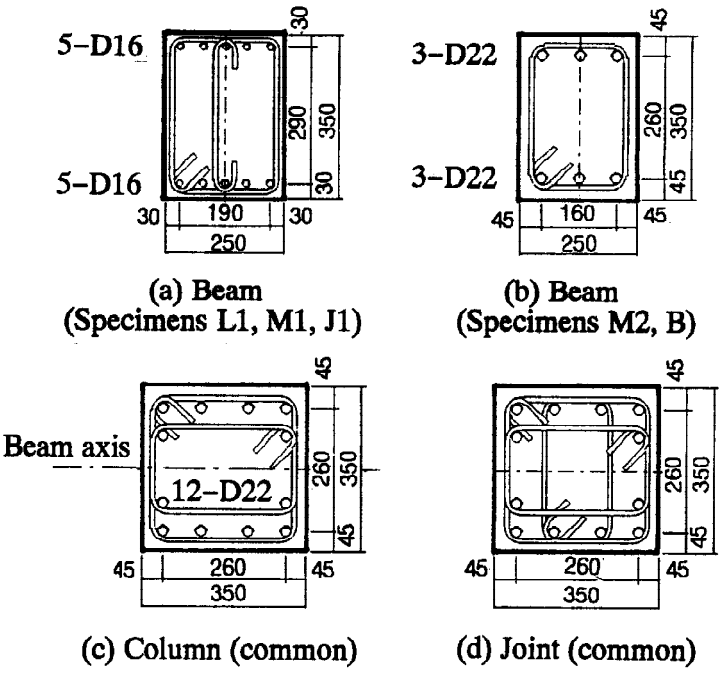

Fig. 1. Member sections (unit in mm)

a_t : total area of tensile reinforcement, p_t : tensile reinforcement ratio,
a_g : total area of longitudinal reinforcement, p_g : gross reinforcement ratio,
p_w : shear reinforcement ratio,
a_w : total area of web reinforcement placed between top and bottom beam reinforcement in the joint,
P_{wj} : ratio of total sectional area of lateral reinforcement to the product of column width and distance between top and bottom beam bar.

Table 2. Material properties

(a) steel

	yielding stress MPa	yielding strain μ	tensile strength MPa	fracture strain %
D10	409	2326	539	18.9
D16	346	1838	518	29.9
D22	363	1884	533	31.9

(b) concrete

	compressive strength MPa	tensile strength MPa	Ec $\times 10^4$ MPa
L1,J1	43	3.2	3.4
M1,M2	44	3.4	3.4
B	47	3.5	3.4

Ec : Secant modulus at one-quarter of the compressive strength.

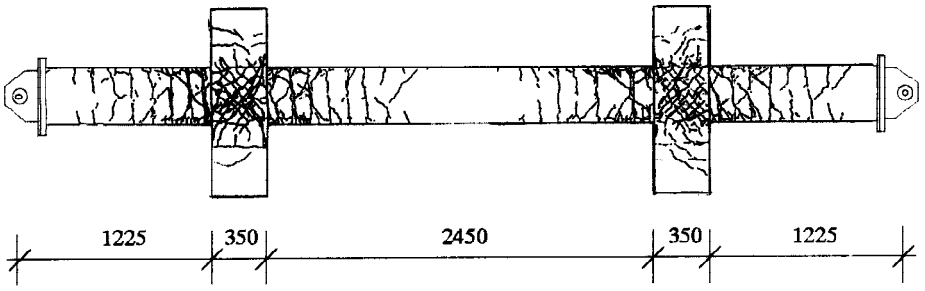

(a) Specimen L1

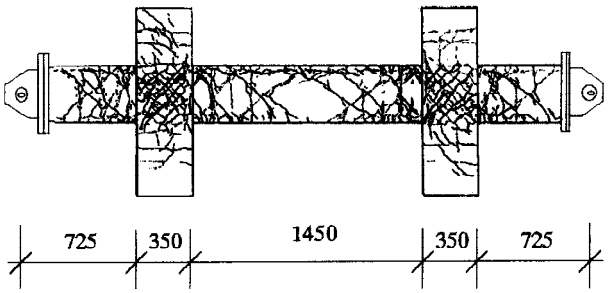

(b) Specimen M1

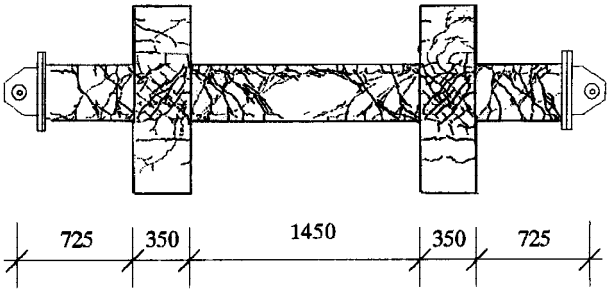

(d) Specimen M2

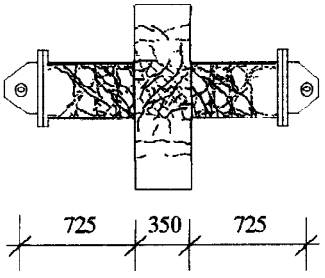

(c) Specimen J1

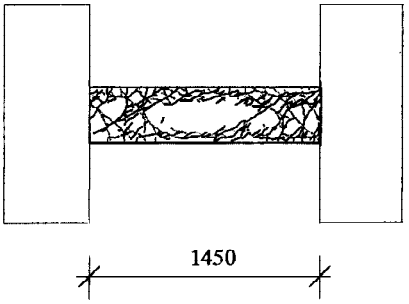

(e) Specimen B

Fig. 2. Configurations of specimens and crack patterns after test

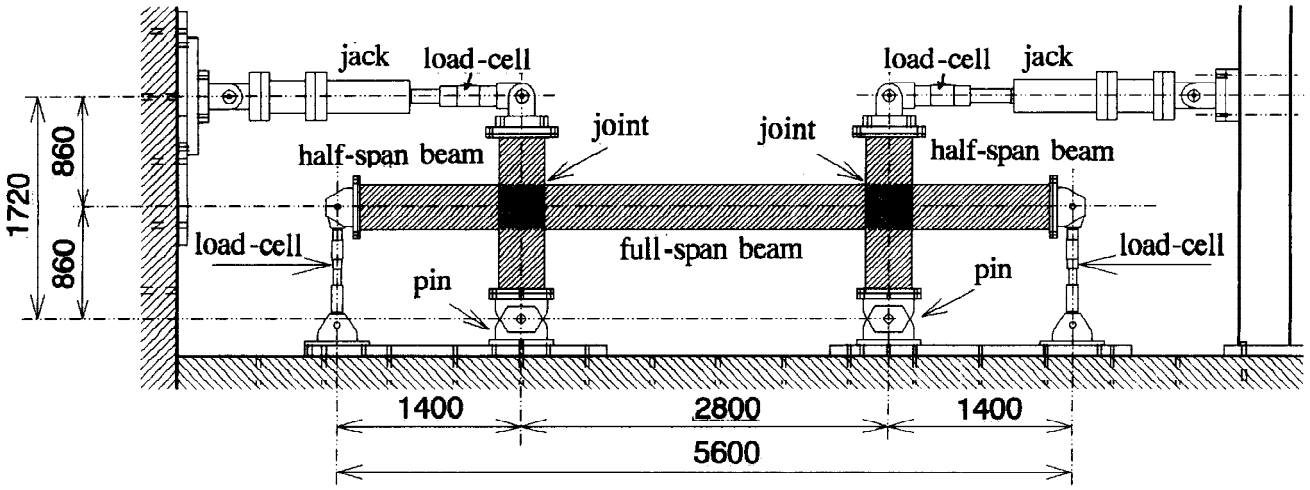

(a) Subassemblage specimens

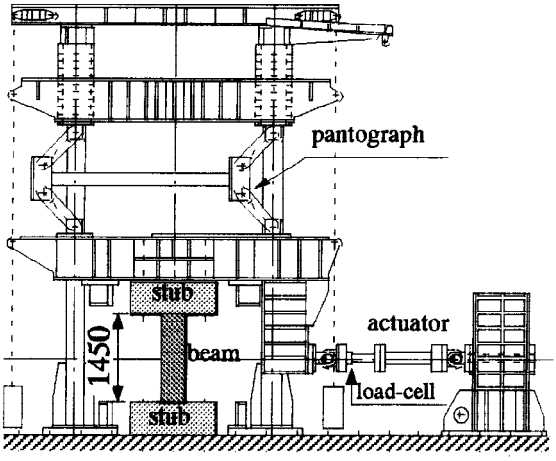

(b) Beam specimen

Fig. 3. Loading apparatuses

TEST RESULTS

General Observations

Crack patterns at the test end are shown in Fig. 2. Many diagonal shear cracks were observed in beam–column joints; however, joints did not fail in shear. Beam bars yielded in subassemblage specimens at the story drift angle, which is defined as the story drift divided by the height(=1720 mm), of 1/100 to 1/80 rad. Joint lateral reinforcement in only Specimen L1 yielded. Splitting cracks along the beam reinforcement of the long full–span beam in Specimen L1 occurred in beam end regions. However these cracks did not spread to the center of the beam. On the other hand, splitting cracks along overall length of beam bars developed in the short full–span beam in Specimens M1 and M2.

The beam bars in Specimen B yielded at the deflection angle of 1/80 rad. Splitting cracks occurred along the top and bottom beam reinforcement, and opened more widely than those of the full–span beam in Specimen M2. The beam eventually failed by the decay of bond transfer ability at the deflection angle of 1/30 rad.

Displacement Contribution

The contribution of parts of Specimen M1 to the story drift is shown in Fig. 4. The contribution in other subassemblage Specimens L1, M2 and J1 was almost similar to that in Specimen M1. The beam component includes the additional deformation due to bar slip. The deflection of beams shared three–quarter of the total story drift. Behavior of beams dominated the general characteristics of these specimens.

Hysteretic Characteristics

The shear – deflection relations for the full-span beam of Specimens L1, M1, M2 and B and the half-span beam of Specimen J1 are shown in Fig. 5. The shear force of the full-span beam in subassemblage specimens is not able to measure directly. Then the beam shear was computed based on the equilibrium of forces acting on the free-body as shown in Fig. 6 which is the half of the full-span beam cut at the center. It was assumed that the contraflexure point where the bending moment is always zero was located in the center of the full-span beam. The shear at beam longitudinal bar yielding for Specimen M1 increased to 1.2 times the half-span beam shear for Specimen J1 since axial load to the full-span beam resulted from the confinement by two columns at beam ends. The axial load increased with the beam deflection and reached to 215 kN. The hysteretic loop in Specimen L1 was spindle-shaped and the dissipating energy was greater than that in Specimen M1. This was attributed to the bar bond deterioration within the entire full-span beam in Specimen M1. The strength of subassemblage specimens was kept almost constant in spite of the damage of the concrete at beam critical sections due to flexural compression.

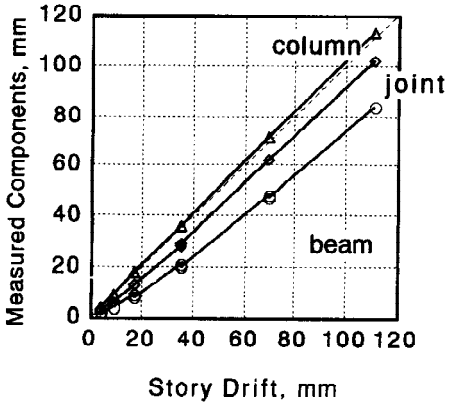

Fig. 4. Deflection components of story drift in Specimen M1

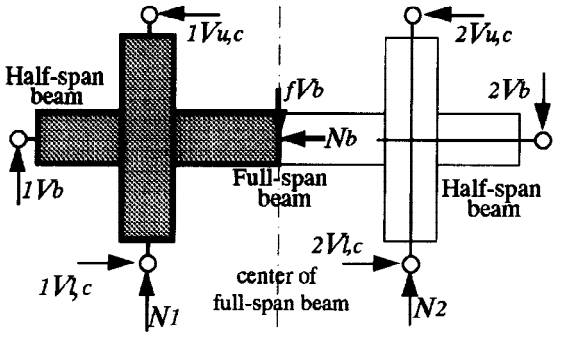

$^1V_{u,c}$, $^2V_{u,c}$: Upper column shear (measured),
^1V_b, ^2V_b : Half-span beam shear (measured),
$^1V_{l,c}$, $^2V_{l,c}$: Lower column shear (computed),
N_1, N_2 : Axial load to lower column (computed),
fV_b : Full-span beam shear (computed),
N_b : Axial load to full-span beam (computed).

Fig. 6. Forces acting on free-body as the half of Specimens L1, M1 and M2

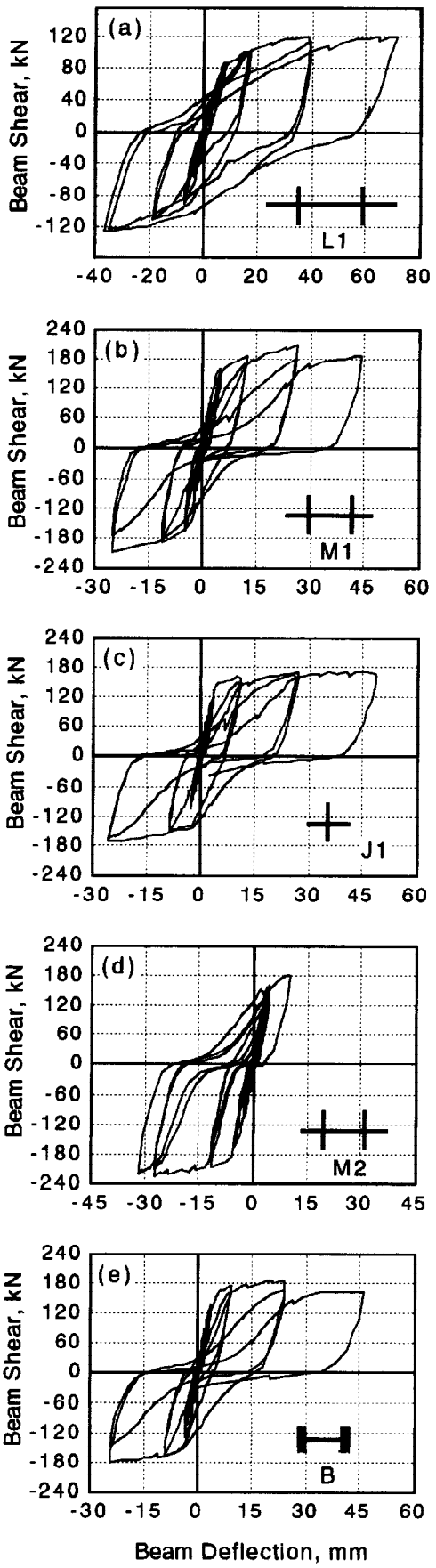

Fig. 5. Beam shear – deflection relations

Strain Distribution along Beam Bar

The strain distribution along top beam reinforcement is shown in Fig. 7 for Specimens L1, M2 and B. Beam deflection angles are pointed out in Fig. 7. The strain of the beam bar in Specimen M2 moved to tension at the column face subjected to compression with the increase in the beam deflection because the bond deterioration occurred along the beam bar within a joint. The beam bar strain at the center of the long full-span beam in Specimen L1 remained almost zero to the test end, while the zero-crossing point of the beam bar strain in short full-span beam of Specimen M2 shifted to compression side (i.e., left side in Fig. 7(b)) with the increase in the beam deflection. However the beam bar strain within the left region of the zero-crossing point in Specimen M2 was kept to be compression. This indicates that the beam reinforcing bar was developed to some extent in the compression region near a plastic hinge of the full-span beam.

The strain distribution along the beam reinforcing bar whose ends were anchored sufficiently in R/C stubs in Specimen B was different from that in Specimen M2. The strain of a beam bar stayed in compression at the critical section under compression.

Beam Bar Slip in Beam-Column Joint

The slip of top beam reinforcement relative to surrounding concrete at the center of a beam-column joint is shown in Fig. 8 for Specimens L1, M1 and J1 to investigate the influence of the beam bar bond deterioration within a full-span beam on the slip behavior of beam bars within a joint. The rotation angle of the hinge region was used as the ordinate.

The beam reinforcement was developed well at the center of the full-span beam of Specimen L1 as indicated in Fig. 7(a) and was welded to the anchorage plate at beam ends in Specimen J1. On the other hand, the bond deterioration due to splitting cracks along the top bars in the full-span beam of Specimen M1 resulted in excessive slip of beam bars within the full-span beam. This is the reason why the beam bar slip within a joint in Specimen M1 was smallest among three specimens comparing at the same hinge rotation angle. This shows the interaction of beam bar bond deterioration within a beam-column joint and a full-span beam.

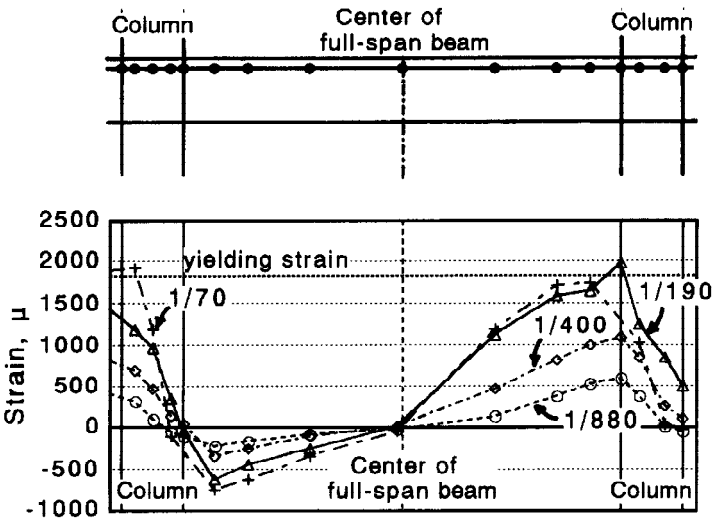

(a) Specimen L1

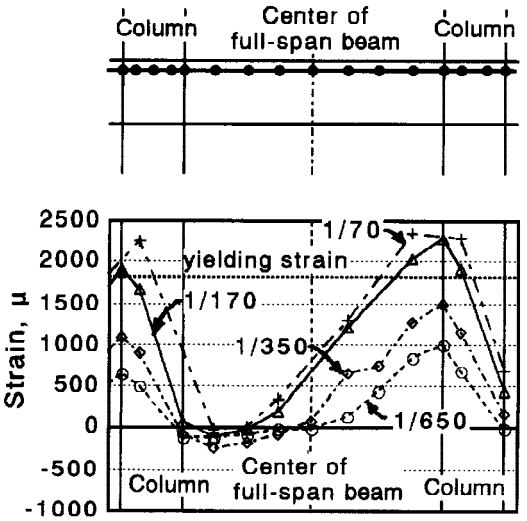

(b) Specimen M2

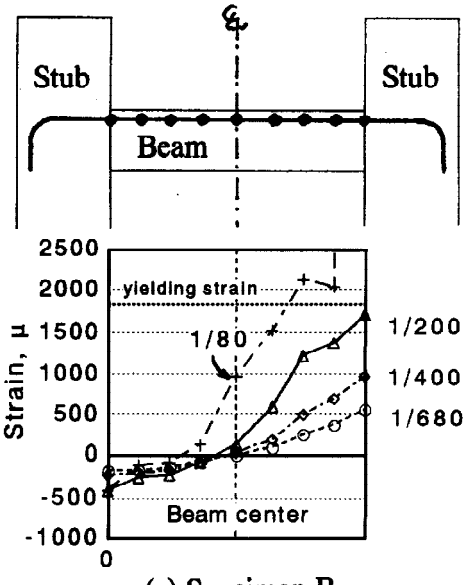

(c) Specimen B

Fig. 7. Strain distributions along top beam bar

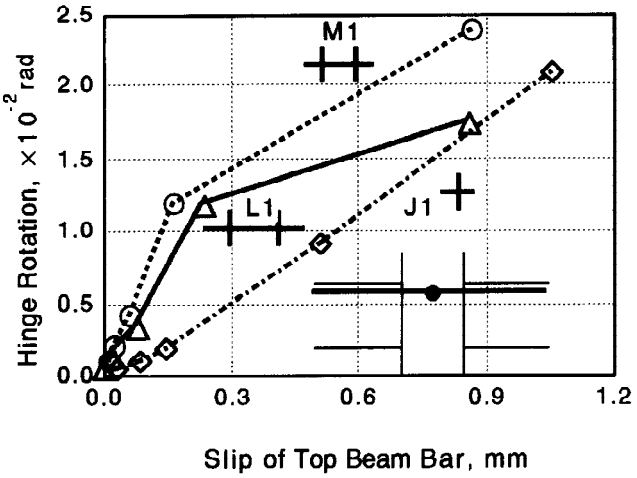

Fig. 8. Slip of top beam bar at center of beam–column joint

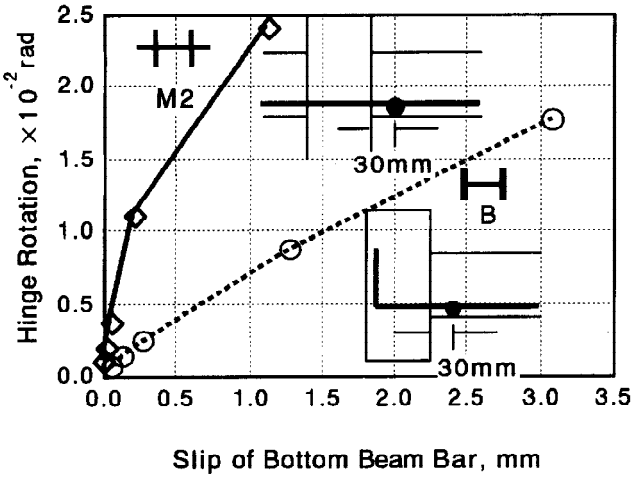

Fig. 9. Slip of bottom beam bar at hinge region of full–span beam

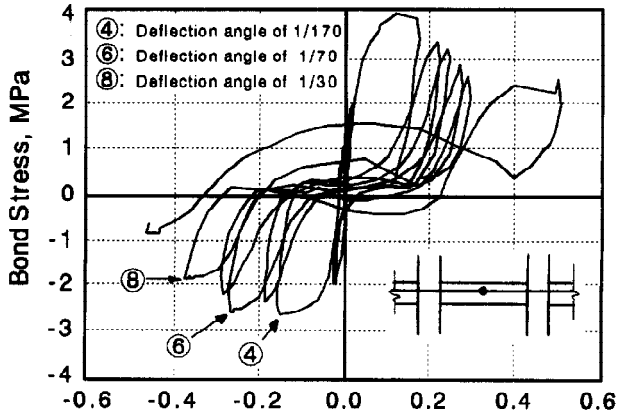

(a) Specimen M2

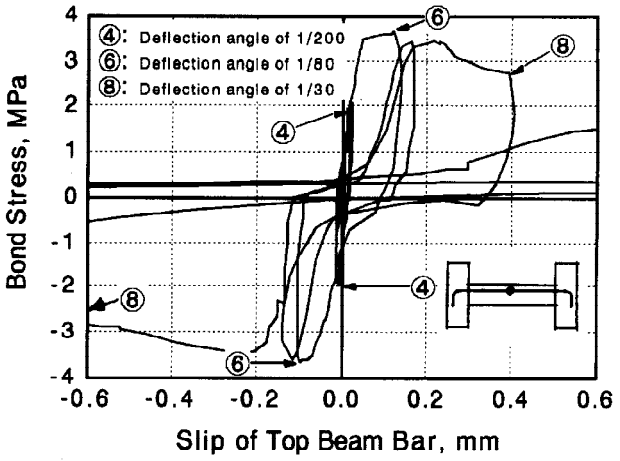

(b) Specimen B

Fig. 10. Beam bar bond stress – slip relations at center of full–span beam

Beam Bar Slip and Bond in Full–Span Beam

The slip of bottom beam reinforcement relative to surrounding concrete at 30 mm apart from the critical section is shown in Fig. 9 for Specimens M2 and B. The beam bar in the full–span beam of two specimens slipped toward the critical section. The beam bar slip at hinge region in the full–span beam of Specimen M2 was small because the pull–out of the beam bar from an adjacent beam–column joint occurred remarkably due to bond deterioration within a joint. On the contrary, the slip at hinge region of Specimen B became quite large because of the small amount of the pull–out of the beam bar from an anchorage stub.

Bond stress along the top beam bar – slip relations at the center of the full–span beam of Specimens M2 and B are shown in Fig. 10. The bond strength within the beam bar length of 400 mm was almost equal for two specimens, i.e., 3.4 MPa approximately which was comparable to the bond strength calculated according to *Design Guidelines for Earthquake Resistant R/C Buildings Based on Ultimate Strength Concept* by Architectural Institute of Japan in 1990. The bond stress in Specimen M2 reached the strength during the fourth loading cycle at the beam deflection angle of 1/170 rad, which was smaller than the corresponding deflection angle in Specimen B. The bond strength in Specimen B started to diminish with the appearance of splitting cracks along beam bars after the seventh loading cycle at the beam deflection angle of 1/80 rad. The beam bar slip at the center of the full–span beam of Specimen B increased rapidly during the eighth loading cycle at the deflection angle of 1/30 rad comparing with that of Specimen M2.

CONCLUDING REMARKS

The following conclusions were drawn from the test results in the paper.

(1) The bond deterioration along the beam reinforcement within an interior beam–column joint and a full–span beam influenced each other. The larger the slip of beam longitudinal bars within a joint was, the smaller that within a full–span beam was.

(2) The beam bar strain of the short full–span beam in a R/C frame remained to be compression at the compression side within a plastic hinge region although the bond deteriorated along the beam bar within an adjacent beam–column joint. The beam bars could be developed to some extent in the full–span beam.

(3) The bond strength along beam bars at the center of the full–span beam was almost equal between the one case where the beam bar ends were anchored sufficiently in stubs using hooks and the other case where beam bar ends passed through interior beam–column joints. The beam bar slip, however, in the full–span beam toward the critical section subjected to tension in former case became quite larger than that in later case. The beam bars within an adjacent beam–column joint slipped as well toward the critical section. This moderated the excessive slip of the beam bars in the full–span beam.

ACKNOWLEDGEMENTS

Authors wish to express their gratitude to Tokyo Metropolitan University, Maeda Memorial Foundation for Engineering Promotion and Yahagi Construction for kindly supports to the study. Authors are grateful to the assistance provided by Mr. S. Minami, research associate in Tokyo Metropolitan University, and the students in Kitayama Laboratory.

REFERENCES

Architectural Institute of Japan (1990). *Design Guidelines for Earthquake Resistant Reinforced Concrete Buildings Based on Ultimate Strength Concept.*, Architectural Institute of Japan, Tokyo.